Available online at www.sciencedirect.com
SCIENCE DIRECT®
Journal of Molecular Structure 695–696 (2004) 189–202
Journal of MOLECULAR STRUCTURE
www.elsevier.com/locate/molstruc

New gas phase reaction to iodine azide, IN_3: microwave spectrum and structure

H.-O. Munz, H.-K. Bodenseh*, M. Ferner

Fakultät für Naturwissenschaften, Abteilung Chemische Physik, Universität Ulm, Ulm D-89069, Germany

Received 14 October 2003; accepted 17 December 2003

Abstract

The unstable molecule iodine azide has been prepared for the first time by a gas phase reaction in a flow system, and the microwave spectra of two isotopic species, a- and b-type, have been measured: the abundant species in the frequency range from 10 to 40 GHz, the $I^{14}N^{15}N^{14}N$-species from 20 to 26 GHz. Rotational constants and centrifugal distortion parameters were obtained. The molecule has been shown to be planar, and the structure was derived. Also, the I-quadrupole coupling constants have been determined.

Keywords: Iodine azide; Microwave spectroscopy; Nuclear quadrupole coupling constants; Molecular structure

1. Introduction

IN_3 has first been synthesized in 1900 by Hantzsch [1] as a highly explosive solid. The reaction was carried out in solution by adding iodine, dissolved in diethylether, to a suspension of silver azide in water; but no good data could be obtained because of poor purity. Only in 1993, Klapötke and co-workers [2] published a modified preparation by using $CFCl_3$ as a solvent, yielding highly pure, bright yellow crystals, suitable for X-ray crystallography. Also, ab initio calculations were carried out [2], spectroscopic work was done with IR [3], ^{14}N NMR [4] and Raman [5]. Furthermore, a structure determination by electron diffraction was published [6]. Following Klapötke's suggestion, we tried to obtain a rotational spectrum, the first samples being supplied in solution over dry ice by his group. By pumping-off the solvent and warming up to $-40\,^{\circ}C$, we could record a reasonable-looking microwave spectrum, showing the typical hyperfine sextets of the iodine nucleus. We then prepared our own crystals, yielding an identical spectrum. We seemingly succeeded in assigning 18 transitions [7], but no other line of the rich spectrum matched these first ones on the basis of a reasonable structure. We finally realized that the spectrum originated from an unknown reaction product of IN_3 and a deposit in the cell from previous measurements. In new, clean metal cells, aluminum or brass, no lines could be found. Obviously, the decomposition was faster than the filling of the cell at the low temperature. We therefore, looked for another way to produce the molecule.

2. Experimental procedures

2.1. Chemical preparation of iodine azide

2.1.1. Parent molecule $I^{14}N_3$

Taking into account the analogy between iodine azide and the isoelectronic molecule iodine isocyanate, we tried the same gas phase reaction as used for the production of INCO [8] according to:

$$AgN_3 + I_2 \rightarrow AgI + IN_3$$

Although, such an approach to obtain a gaseous azide had never been reported before, the attempt was immediately successful: iodine vapour was passed in a flow system over silver azide at 120 °C (optimum temperature) and through the absorption cell, maintaining a total pressure of 2–3 Pa for survey spectra and 0.6 Pa for frequency measurements.

* Corresponding author. Address: c/o Abteilung Quanteninformationsverarbeitung, Universität Ulm, Ulm D-89069, Germany. Tel.: +49-731-502-2832; fax: +49-731-502-2839.
E-mail address: hans-karl.bodenseh@chemie.uni-ulm.de (H.-K. Bodenseh).

0022-2860/$ - see front matter © 2004 Elsevier B.V. All rights reserved.
doi:10.1016/j.molstruc.2003.12.045

The products were trapped behind the cell by LN_2. An intense microwave spectrum was obtained which could easily be ascribed to iodine azide and assigned in a straightforward manner. Silver azide was precipitated by adding an aqueous solution of silver nitrate to a solution of sodium azide in water, filtered-off, washed with water, ethanol, and finally with diethylether and carefully dried. About 0.1 mol were put into a quartz boat which was placed into a quartz tube of 4 cm in diameter and surrounded by an oven, 30 cm in length and horizontally arranged. Such a charge could be used for more than a week. In spite of intense drying, it was impossible to avoid producing strong transitions of HN_3 so long as IN_3 was produced from a given sample of silver azide. These appeared even at room temperature as soon as the iodine vapour was added, whereas water vapour without iodine over silver azide yielded no trace of HN_3 even at 220 °C: obviously IN_3 has to be formed first and then reacts with water to make HN_3. When steady state is reached in the flow system and the cell is then closed simultaneously at both ends, the strong signals from IN_3 decay with a rate that can be described best by a second order law: after 10 min half intensity is reached and after 50 min nothing more can be detected. While IN_3-crystals produced in solution cannot be cooled down to LN_2-temperature without explosion, we had no problem in trapping the IN_3-vapour at that low temperature as a microcrystalline sublimate. Warming the trap with caution and flowing the products back through the cell, yields at first the spectrum of HN_3 followed by that of IN_3. So the IN_3 produced in the gas phase can be handled much more safely than that produced in solution. Obviously, IN_3 condensed from the gas phase forms a molecular crystal, whereas that from solution forms layers of I–N–I–N-chains [2]. Perhaps, these chains rearrange only slowly, compared to the rate of decomposition in the metal cells, to the monomer molecules. This may also explain why these transitions are about one order of magnitude weaker and not suited for searching the unknown spectrum. As we found out by another preparation in solution, they can be identified if their position is known. But even if the procedures described here appear relatively safe: the usual precautions when handling azides should always be taken! When manipulating the substances, the whole body was at all times protected by a thick leather apron, the eyes by safety glasses, the hands by gloves of chain-mail, and the head by a helmet with additional safety shield in front of the face. The glass traps were contained in Dewar vessels made from stainless steel. As soon as the silver azide had been placed into the reaction tube in the oven, this part of the spectrograph was isolated towards the operators by an acrylic glass shield, 2 cm in thickness and wrapped with several layers of transparent foil against slivering by the impact of a shock wave. While dealing with iodine azide prepared from solution, several detonations occurred, but never with iodine azide prepared from the gas phase.

2.1.2. $I^{14}N^{15}N^{14}N$

$^{15}NH_4^{14}NO_3$ was used as starting material. It was heated for 20 h at 220 °C in an evacuated and sealed glass ampoule to yield ^{15}NNO. After cooling down this was condensed into another, evacuated ampoule over $NaNH_2$. Heating to 300 °C for 22 h resulted in the formation of $Na^+(^{14}N^{15}N^{14}N)^-$ which was converted to the silver salt as described above. Due to the limited supply of the substituted ammonium nitrate, the quantities had to be drastically reduced to mmol scale and the experimental setup was accordingly changed: instead of the horizontal arrangement of oven and reaction tube a vertical one was used with the quartz tube only 2 cm in diameter and 15 cm in length. At about 5 cm from the lower end of the tube a frit was inserted. Because the tube was equipped with ground joints at both ends it could be used instead of a filter and the precipitated silver azide was sucked directly onto the frit, a layer of quartz wool in-between. Washing the salt was done through the tube and the frit, also the first drying. Final drying occurred after insertion into the gas flow line at the spectrometer. A small oven of 10 cm in length was placed around the reaction tube. With this modified setup the optimum temperature for producing IN_3 increased to 160 °C. During the tests to minimize the sample size, we realized that the reaction was not reproducible: 300 mg (~2 mmol) silver azide sometimes allowed spectra to be taken through 3 h, but sometimes only for a few minutes; all intermediate values were possible. We could not find out the reason; it seems to be a surface effect of the crystals depending upon tiny variations in the conditions of precipitation and was not important with the large samples for the parent molecule. So we just had to trust luck when using the ^{15}N-sample.

2.2. Spectrometer setup

The microwave spectrograph was of conventional Stark-type operating at 30 kHz. Because pyrolytic or discharge reactions for producing instable species do not often reach a real steady state and the yield of the desired product can change within seconds, relatively fast time averaging is necessary for good results. Therefore, the apparatus was equipped with a self-configured and -programmed ELTEC© computer based on a MOTOROLA© 68K processor. The original idea was to step the frequency in small increments via a fast switching frequency standard and to have the microwave source, a MARCONI© sweeper, following by means of a phase locking circuit. But because the microwave power incident at the detector diode is not constant vs. frequency, the switching within a few μs produces sharp rises or drops of the voltage across the diode. The harmonics thereof reach easily into the range of the modulation frequency and produce excessive noise in the signal channel. Therefore, a method was chosen which allowed analog sweeping of the microwave source and still kept all the advantages of digital signal processing. A block diagram with the basic elements (no attenuators etc.) of

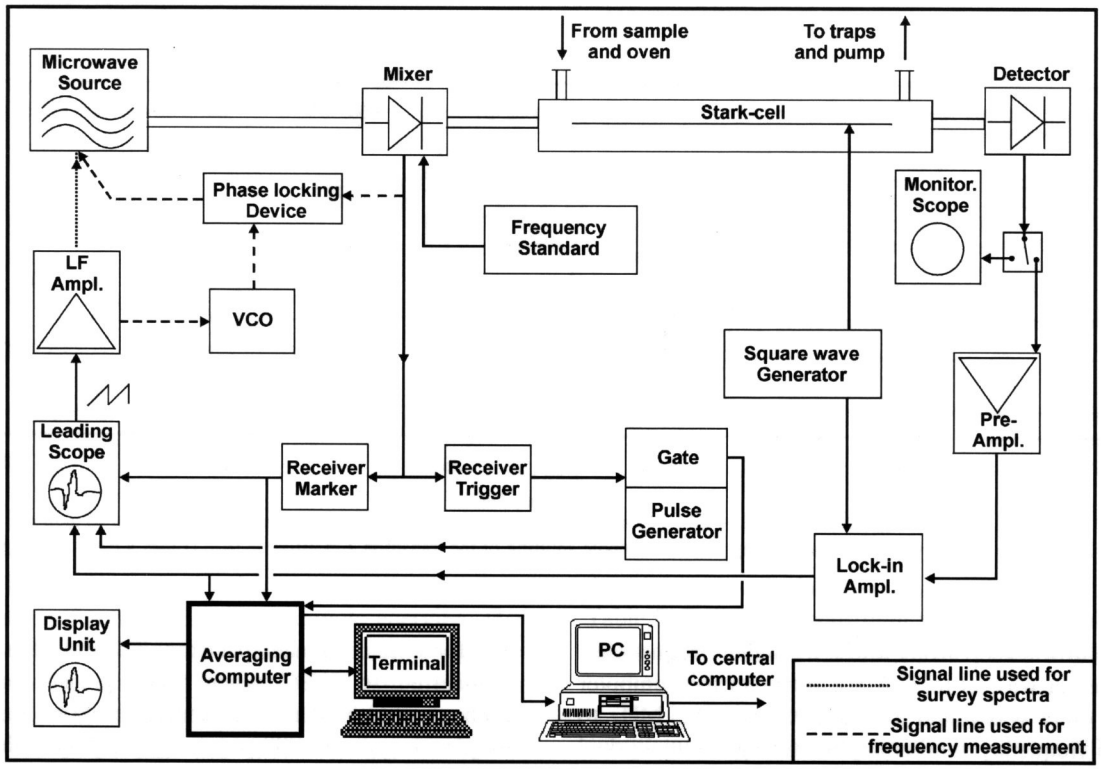

Fig. 1. Simplified block diagram of the spectrograph.

the setup is shown on Fig. 1: a pulse generator triggered a 'leading' scope at the front end of the spectrograph and a monitoring scope (to observe the tuning of the MW-power) at the far end of the cell, the repetition rate was adjustable to match the acquisition time the computer needed for one sweep. The time base (sawtooth) of the leading scope was fed into a special low frequency amplifier to adjust amplitude, offset, and polarity (for sweep reversal). The MW-sweeper with backward wave oscillator plug-ins could be operated in single frequency mode. In this mode, the frequency determining high voltage was especially stabilized, yielding high stability of the output frequency with only small and slow drifts. An FM-input (bandwidth DC-5 MHz) allowed a modulating voltage to be superimposed and was used to sweep the MW-frequency with the adjusted sawtooth for survey spectra or to stabilize the source by the output voltage of a phase locking device for precise frequency measurements.

- For survey spectra a range of 55–60 MHz was chosen. Some db of the MW-power were coupled to a mixing diode and mixed with the harmonics of the frequency standard. The resulting intermediate frequencies were detected by means of two identical commercial, quartz controlled communications receivers, 0.09–34 MHz. One of them was used to trigger the computer. Therefore, it was set to, e.g. 26 MHz and gave a signal when the swept MW-frequency was 26 MHz below or above the corresponding harmonic of the frequency standard. The output had to pass a gate circuit, which was opened by the pulse generator when starting a sweep. The time the gate was open could be adjusted and was chosen to about 1/3 of a sweep duration. Thus, false triggering of the computer by the upper frequency marker was avoided in cases when the lower marker was not caught. The other receiver was tuned to, e.g. 25 MHz and produced two frequency markers with 50 MHz separation for evaluating the frequencies of the absorption lines. Triggering the computer with a real time frequency marker had the effect that sampling always started at the same frequency and that drifts of the un-stabilized sweeper did not blur the accumulated sweeps. The achieved frequency accuracy of 300–500 kHz was sufficient for assignments. Using the frequency markers these spectra could be concatenated with arbitrary frequency scaling for viewing larger spectral ranges.
- For precise frequency measurements we made use of the fact that the width of the band-pass filters in signal- and reference-channel of our phase locking device (FDS 30 by Schomandl©) was about 4 MHz. Instead of offering a fixed frequency of 10 MHz for reference (internally tripled to 30) we drove a voltage-controlled oscillator with the sawtooth voltage from the low frequency amplifier, thus generating a reference frequency which started from 31.5 MHz, decreased linearly to 27.5 MHz, and jumped back. When locked, the MW-frequency had to follow; and when the lower side IF was used, this

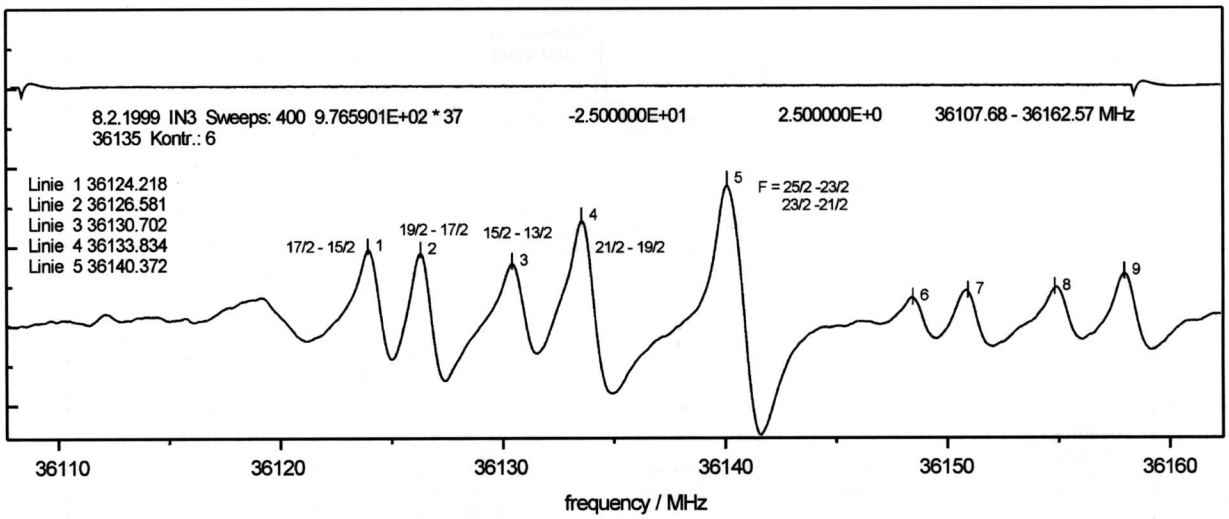

Fig. 2. Example of a survey spectrum showing the I-quadrupole splitting of the transition $J = 10_{1,10} \leftarrow 9_{1,9}$. (Lines # 6–9 not assigned).

resulted in a sweep from lower to higher frequencies. One receiver was set to 31 MHz to trigger the computer and the other was tuned to, e.g. 29.0 and 28.5 MHz to produce frequency markers. This arrangement worked reliably with repetition rates of 9 Hz and sweep durations of 110 ms. Although sweep reversal was provided, it was not necessary to use it except for occasional checking: the parameters could always be adjusted in a way that the full half-width of a line, be it broad or narrow, extended over 1/3 of the sweep width and $\approx$35 ms were needed to sweep over this range. Because the time constant of the lock-in amplifier was set to 1 ms, no time delay could be observed. The frequency standard was monitored against the standard signals of DCF77-station, Mainflingen, Germany, the relative deviations kept $< 10^{-8}$.

As stated, when triggered by the frequency marker of the first receiver, the computer started displaying the output of the lock-in amplifier with the repetition rate of 9 Hz and, when all was correct, the sampling was started. The first value of the A/D-converter was added to the first memory location, then the content was read out and checked if it would not exceed the range of the display. When necessary, the scale factor was changed and the value was displayed as the first point of the spectrum on a screen with medium persistence. This procedure was repeated for all 1000 points of the sweep and then the computer waited for the next trigger marker. Sampling could be interrupted as soon as the *S/N*-ratio was sufficient, or more sweeps could be added to the number initially set. Since, the frequency markers were almost noiseless, it was sufficient to fix the number of sweeps to 10. The accumulated data of the lock-in output were never changed and, as original data, stored as integers with 32 bits. After sampling a menu asked for the setting of the frequency standard, for the harmonic, for the frequencies of the markers, the substance, for the experimental details, and for a name of the spectrum. Then all these data were transferred to a PC where each project had its own exchangeable hard disk. A special program calculated the frequencies of all 1000 points and displayed the spectrum. The peaks could be marked with a cursor, and these frequencies were collected in a list. After passing these extended data to the program ORIGIN© by Microcal Software Inc, the spectrum could be plotted; for frequency determination a fit to Lorentzian line shape was performed. Finally, the collected frequencies were sent to the central computer together with quantum numbers for fitting the spectrum. Fig. 2 and 3 show examples of a survey spectrum and of a frequency determination.

3. Results

3.1. Rotational spectra and spectroscopic constants

The spectrum of the parent molecule was measured from 10 to 40 GHz, the cell temperature kept at -5 °C. Three hundred and fifteen hyperfine transitions belonging to 89 transitions in J_τ, a- and b-type, could be assigned. As mentioned above, this assignment was not difficult: due to the large quadrupole splitting of the I-nucleus the typical a-type pattern of a very near prolate asymmetric top shows up only from higher J-values upward; but then it is very distinct as can be seen from Fig. 4 where 30 survey spectra have been concatenated to show the transition $J = 10 \leftarrow 9$. With these first rough constants, the b-type transitions could be identified. More details are given in Ref. [9]. Because each rotational line represents an unresolved multiplet of the up to 27 hyperfine transitions of the three N-nuclei, the line widths were about 800 kHz even at very low pressures. Nevertheless, the assigned transitions could be fitted with a standard deviation of 62 kHz. The program 'Q2fit' by

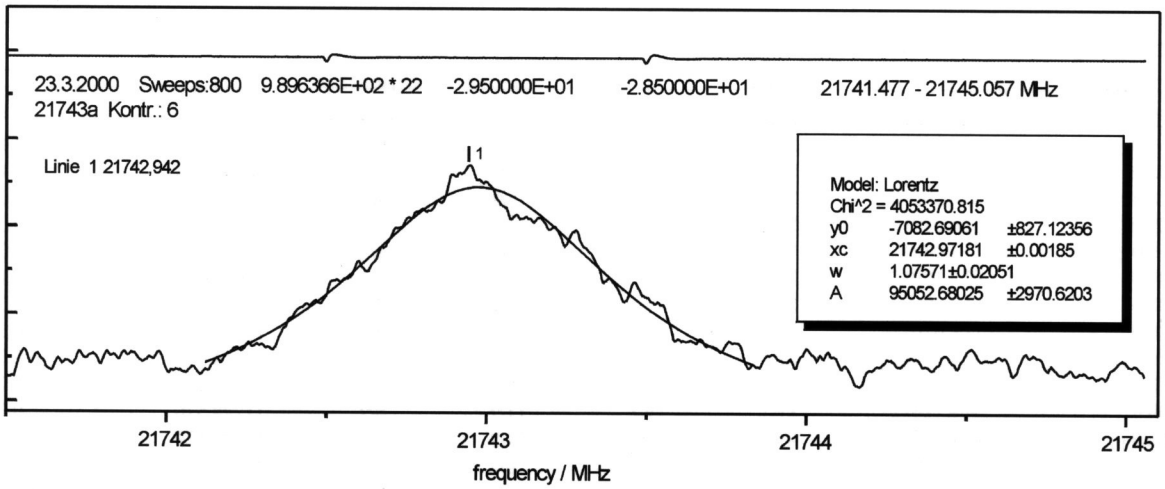

Fig. 3. Example of a frequency determination (the almost coinciding transitions $6_{3,4}$ 17/2 ← $5_{3,3}$ 15/2 and $6_{4,2}$ 9/2 ← $5_{4,1}$ 7/2 of $I^{14}N^{15}N^{14}N$).

Zbigniew Kisie[1] was used which performs complete diagonalization of rotational and quadrupole energies. The transitions were weighted according to their accuracy; the calculations were done with Watson's [10] A-reduction in I^r-representation. Besides the rotational and the five quartic distortion constants, χ_{aa}, $\chi_{bb}-\chi_{cc}$, and χ_{ab} could be determined. The frequencies are given in Table 1, the spectroscopic constants in Table 3. No transitions of low F-values could be found which were isolated enough to measure their Stark-shifts. Therefore, the components of the dipole moment could not be determined. Because the yield of IN_3 and with it the intensity of the transitions was fluctuating, even their ratio could not be estimated from the relative intensities of a- and b-type transitions. Also, due to the splitting of each transition into six lines the spectrum is very rich, and we did not succeed in assigning vibrational satellites.

Because of the small sample of the ^{15}N-substituted species these measurements had to be restricted to the range 20–30 GHz and not as many sweeps could be taken for the frequency measurements as would have been desirable. Therefore, the accuracy of the constants is not comparable to that of the parent molecule. 59 hyperfine transitions, belonging to 19 transitions in J_τ, could be assigned, but only four of b-type among them. They are listed in Table 2. The best results with a standard deviation of 126 kHz were obtained by fitting only the rotational constants, just Δ_J and Δ_{JK} for the distortion constants, and two of the three quadrupole quantities: χ_{cc} should not be affected by the rotation of the a–b-plane around the c-axis, and the small change of χ_{bb} by the substitution could be estimated with sufficient accuracy. Therefore, $\chi_{bb} - \chi_{cc}$ was held constant, and the remaining three distortion constants were also fixed to the values of the parent molecule. The slightly reduced accuracy of the rotational constants is not detrimental to the structure calculations. All constants are included in Table 3. Due to the constraint for the trace of the coupling tensor the values for χ_{bb} and χ_{cc} have been slightly changed by the fitting process.

The substitution of the central N-atom had been complete: no lines of the parent molecule could be detected.

3.2. Nuclear quadrupole coupling

As mentioned, only the coupling of the ^{127}I-nucleus is considered, the splitting due to the ^{14}N-nuclei remaining unresolved. Because χ_{ab} results directly from the spectrum along with χ_{aa} and χ_{bb}, the planar problem can easily be diagonalized to yield the principal values of the quadrupole coupling tensor. They are given in Table 4 together with the angle φ between a-inertial axis and the z-principal quadrupole axis. This angle, a byproduct from the diagonalization, is an essential quantity for the structure

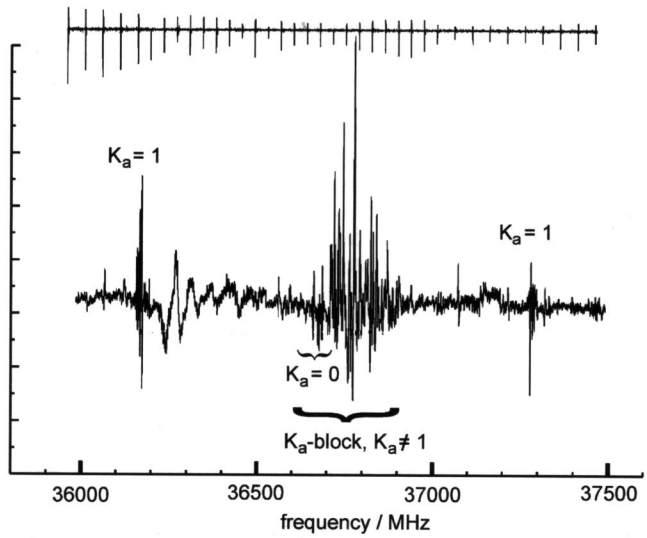

Fig. 4. Wide range spectrum of the transition $J = 10 \leftarrow 9$ (30 survey spectra concatenated).

[1] Institute of Physics, Polish Academy of Sciences, Al. Lotnikow 32/46, Warsaw, Poland.

Table 1
Rotational transitions of $I^{14}N_3$ (frequencies in MHz)

J'	K_a'	K_c'	J''	K_a''	K_c''	F'	F''	Frequency	o–c
3	1	3	2	1	2	7/2	5/2	10744.606	−0.107
						9/2	7/2	10797.318	0.174
						7/2	7/2	10805.166	−0.018
						11/2	9/2	10881.389	0.007
3	0	3	2	0	2	3/2	1/2	10834.824	−0.060
						7/2	5/2	10948.090	−0.137
						11/2	9/2	11035.041	0.071
						9/2	7/2	11051.404	−0.004
3	1	2	2	1	1	7/2	5/2	11114.356	−0.052
						9/2	7/2	11137.270	−0.082
						11/2	9/2	11228.576	−0.051
4	1	4	3	1	3	7/2	5/2	14395.629	−0.043
						9/2	7/2	14427.230	0.029
						11/2	9/2	14473.617	0.053
						13/2	11/2	14499.276	0.048
4	0	4	3	0	3	7/2	5/2	14608.735	−0.134
						9/2	7/2	14653.825	−0.110
						9/2	9/2	14660.925	0.010
						13/2	11/2	14694.976	0.039
4	2	2	3	2	1	9/2	9/2	14598.691	−0.102
						9/2	7/2	14607.473	0.022
						11/2	9/2	14617.819	−0.002
						7/2	5/2	14657.356	−0.043
						13/2	11/2	14758.561	0.055
4	2	3	3	2	2	9/2	9/2	14595.205	0.059
						9/2	7/2	14603.994	0.118
						11/2	9/2	14614.365	−0.030
						7/2	5/2	14653.825	−0.095
						13/2	11/2	14755.630	0.019
4	3	1,2	3	3	0,1	11/2	9/2	14510.656	0.026/0.030
						9/2	7/2	14521.354	0.109/0.115
						7/2	5/2	14701.463	0.056/0.052
4	1	3	3	1	2	11/2	11/2	14715.340	0.112
						7/2	5/2	14864.659	0.032
						9/2	7/2	14875.237	0.015
						9/2	9/2	14900.773	0.066
						13/2	11/2	14932.696	−0.027
5	1	5	4	1	4	9/2	7/2	18035.426	0.030
						11/2	9/2	18058.165	−0.044
						13/2	11/2	18086.921	0.043
						15/2	13/2	18095.954	−0.007
5	0	5	4	0	4	15/2	13/2	18357.708	0.077
						11/2	9/2	18363.398	0.218[a]
						13/2	11/2	18363.398	0.029
5	2	3	4	2	2	11/2	9/2	18317.586	0.043
						13/2	11/2	18336.769	−0.011
						15/2	13/2	18402.416	0.027
5	2	4	4	2	3	11/2	9/2	18310.586	−0.096
						9/2	7/2	18320.977	−0.120
						13/2	11/2	18330.209	0.074
						7/2	5/2	18355.667	0.009
						15/2	13/2	18396.388	0.001
5	3	2,3	4	3	1,2	11/2	9/2	18266.643	0.053/0.067
						13/2	11/2	18284.163	0.056/0.070
						15/2	13/2	18438.863	−0.062/−0.073
5	1	4	4	1	3	7/2	9/2	18606.417	−0.063
						11/2	9/2	18616.230	−0.042
						13/2	11/2	18634.310	0.007
						15/2	13/2	18649.475	0.058
6	1	6	5	1	5	9/2	7/2	21660.085	−0.027
						11/2	9/2	21662.623	−0.078

(continued on next page)

Table 1 (*continued*)

J'	K_a'	K_c'	J''	K_a''	K_c''	F'	F''	Frequency	o−c
						13/2	11/2	21679.796	0.057
						7/2	5/2	21679.831	−0.040
						15/2	13/2	21699.046	0.002
						17/2	15/2	21702.328	−0.021
6	0	6	5	0	5	9/2	7/2	21980.661	0.021
						11/2	9/2	21986.197	−0.042
						7/2	5/2	21994.470	−0,008
						13/2	11/2	22002.820	0.006
						17/2	15/2	22020.565	0.027
						15/2	13/2	22022.834	−0.055
6	2	4	5	2	3	13/2	11/2	22010.974	−0.072
						15/2	13/2	22027.484	−0.062
						9/2	7/2	22027.484	0.250[a]
						7/2	5/2	22060.091	−0.052
						17/2	15/2	22062.169	−0.027
6	2	5	5	2	4	13/2	11/2	21999.288	−0.021
						15/2	13/2	22016.121	0.029
						9/2	7/2	22016.121	0.134[a]
						17/2	15/2	22051.501	0.009
6	3	3,4	5	3	2,3	13/2	11/2	21976.146	0.017/0.052
						15/2	13/2	21995.590	−0.003/0.032
						11/2	9/2	21997.640	0.030/0.065
						9/2	7/2	22044.854	0.009/0.041
						17/2	15/2	22081.052	−0.052/−0.022
6	4	2,3	5	4	1,2	15/2	13/2	21963.378	−0.091
						11/2	9/2	21989.930	−0.008
						17/2	15/2	22117.140	−0.019
6	5	1,2	5	5	0,1	13/2	11/2	21888.697	0.056
						15/2	13/2	21925.469	−0.075
6	1	5	5	1	4	11/2	9/2	22343.503	−0.049
						9/2	7/2	22346.438	−0.033
						13/2	11/2	22348.710	0.078
						7/2	5/2	22354.123	−0.050
						15/2	13/2	22361.395	−0.058
						17/2	15/2	22372.798	−0.029
7	1	7	6	1	6	11/2	9/2	25280.638	0.018
						13/2	11/2	25283.584	0.022
						9/2	7/2	25294.464	0.114
						15/2	13/2	25296.668	0.041
						17/2	15/2	25310.382	−0.014
						19/2	17/2	25311.399	0.025
7	0	7	6	0	6	11/2	9/2	25651.709	0.010
						9/2	7/2	25658.898	−0.020
						13/2	11/2	25660.558	0.001
						15/2	13/2	25672.644	0.019
7	3	4,5	6	3	3,4	15/2	13/2	25668.425	−0.030/0.048
						13/2	11/2	25676.553	−0.091/−0.014
						17/2	15/2	25684.997	−0.085/−0.009
						11/2	9/2	25703.615	−0.145/−0.072
						19/2	17/2	25736.434	−0.142/−0.074
7	4	3,4	6	4	2,3	15/2	13/2	25645.380	−0.005
						17/2	15/2	25667.727	0.004
						13/2	11/2	25669.692	−0.015
						11/2	9/2	25722.630	−0.103/−0.096
						19/2	17/2	25761.773	−0.015
7	5	2,3	6	5	1,2	15/2	13/2	25616.543	−0.002
						17/2	15/2	25647.436	−0.011
						13/2	11/2	25661.535	0.060
7	6	1,2	6	6	0,1	15/2	13/2	25581.336	−0.029
7	1	6	6	1	5	9/2	7/2	26077.898	−0.084
						15/2	13/2	26080.522	0.028
						17/2	15/2	26090.590	−0.021

(*continued on next page*)

Table 1 (*continued*)

J'	K_a'	K_c'	J''	K_a''	K_c''	F'	F''	Frequency	o−c
						13/2	11/2	26103.118	−0.024
						19/2	17/2	26120.640	0.014
						11/2	9/2	26120.640	0.162[a]
8	1	8	7	1	7	13/2	11/2	28897.876	−0.058
						15/2	13/2	28900.668	−0.087
						11/2	9/2	28908.052	0.040
						17/2	15/2	28911.078	0.038
						21/2	19/2	28921.391	0.080
						19/2	17/2	28921.391	0.064
8	0	8	7	0	7	13/2	11/2	29288.265	−0.019
						19/2	17/2	29312.285	−0.051
						15/2	13/2	29322.085	−0.080
						17/2	15/2	29330.433	−0.054
						21/2	19/2	29342.620	0.053
8	1	7	7	1	6	13/2	11/2	29693.680	−0.009
						21/2	19/2	29721.076	−0.031
						15/2	13/2	29723.313	−0.038
						17/2	15/2	29790.561	−0.016
						19/2	17/2	29794.161	0.028
						11/2	9/2	29801.557	−0.137
8	2	6	7	2	5	17/2	15/2	29381.258	0.070
						13/2	11/2	29381.258	−0.083
8	3	5,6	7	3	4,5	15/2	13/2	39354.829	−0.089/0.063
						19/2	17/2	29365.656	−0.117/0.032
8	4	4,5	7	4	3,4	19/2	17/2	29356.190	−0.021
						13/2	11/2	29383.090	−0.109
8	5	3,4	7	5	2,3	21/2	19/2	29442.683	0.009
9	1	9	8	1	8	15/2	13/2	32512.972	−0.013
						17/2	15/2	32515.539	−0.001
						13/2	11/2	32520.676	−0.042
						19/2	17/2	32523.844	0.009
						23/2	21/2	32531.473	0.080
						21/2	19/2	32531.874	0.048
9	0	9	8	0	8	17/2	15/2	32998.613	−0.057
						23/2	21/2	33000.385	−0.002
						19/2	17/2	33009.256	−0.036
						15/2	13/2	33056.793	−0.086
						21/2	19/2	33090.699	−0.012
						13/2	11/2	33091.270	−0.054
9	1	8	8	1	7	13/2	11/2	33524.780	0.019
						19/2	17/2	33527.377	0.033
						21/2	19/2	33534.035	−0.001
						17/2	15/2	33536.562	−0.067
						23/2	21/2	33557.225	−0.013
10	1	10	9	1	9	17/2	15/2	36126.223	−0.013
						19/2	17/2	36128.505	0.014
						15/2	13/2	36132.439	0.026
						21/2	19/2	36135.388	0.048
						25/2	23/2	36141.247	0.051
						23/2	21/2	36141.783	0.001
10	0	10	9	0	9	17/2	15/2	36628.862	0.030
						15/2	13/2	36630.110	−0.030
						23/2	21/2	36630.676	−0.025
						19/2	17/2	36642.934	−0.013
						21/2	19/2	36647.591	0.046
						25/2	23/2	36655.497	0.046
10	1	9	9	1	8	19/2	17/2	37246.767	0.175[a]
						17/2	15/2	37246.767	−0.003[a]
						15/2	13/2	37246.767	−0.109[a]
						21/2	19/2	37247.879	−0.038
						23/2	21/2	37252.824	0.037
						25/2	23/2	37258.240	−0.015
11	1	11	10	1	10	19/2	17/2	39737.815	−0.030

(*continued on next page*)

Table 1 (*continued*)

J'	K_a'	K_c'	J''	K_a''	K_c''	F'	F''	Frequency	o−c
						21/2	19/2	39739.805	0.006
						17/2	15/2	39743.099	0.093
						23/2	21/2	39745.634	0.011
						27/2	25/2	39750.498	0.045
						25/2	23/2	39751.074	0.010
11	0	11	10	0	10	19/2	17/2	40293.380	−0.007
2	1	1	2	0	2	3/2	1/2	28785.962	−0.116
3	1	2	3	0	3	3/2	1/2	29016.202	−0.052
						9/2	9/2	29374.651	−0.003
4	1	3	4	0	4	7/2	7/2	29551.941	−0.035
						11/2	11/2	29570.640	0.029
						9/2	9/2	29591.536	−0.065
5	1	4	5	0	5	5/2	5/2	29686.730	0.010
						15/2	15/2	29735.045	0.023
						9/2	9/2	29818.028	−0.075
						13/2	13/2	29841.541	−0.004
6	1	5	6	0	6	7/2	7/2	30046.310	−0.129
						17/2	17/2	30087.360	0.050
						9/2	9/2	30130.604	0.066
						15/2	15/2	30180.239	0.129
						13/2	13/2	30190.550	0.038
7	1	6	7	0	7	9/2	9/2	30465.511	0.008
						19/2	19/2	30525.525	0.024
						17/2	17/2	30591.126	0.083
						15/2	15/2	30598.557	0.176
						11/2	11/2	30599.370	0.083
						13/2	13/2	30618.088	0.087
8	1	7	8	0	8	21/2	21/2	30904.142	0.100
						11/2	11/2	30989.737	0.082
						15/2	15/2	31019.217	0.031
						17/2	17/2	31058.502	0.033
9	1	8	9	0	9	13/2	13/2	31423.104	0.012
						23/2	23/2	31460.936	0.044
						15/2	15/2	31484.422	−0.051
						21/2	21/2	31516.287	0.123
						17/2	17/2	31554.762	0.100
						19/2	19/2	31576.586	0.063
10	1	9	10	0	10	15/2	15/2	32039.836	0.007
						25/2	25/2	32063.766	0.069
						17/2	17/2	32102.396	−0.015
						23/2	23/2	32138.230	−0.019
						19/2	19/2	32158.315	0.009
						21/2	21/2	32176.868	−0.026
11	1	10	11	0	11	17/2	17/2	32710.761	−0.002
						27/2	27/2	32731.796	0.027
						19/2	19/2	32773.950	0.099
						25/2	25/2	32808.932	0.049
						23/2	23/2	32842.276	0.087
12	1	11	12	0	12	19/2	19/2	33456.826	0.052
						27/2	27/2	33547.678	0.033
						23/2	23/2	33582.086	0.086
						25/2	25/2	33593.038	0.014
13	1	12	13	0	13	21/2	21/2	34265.983	0.072
						31/2	31/2	34280.931	−0.034
						23/2	23/2	34334.801	−0.032
						29/2	29/2	34359.349	0.051
						27/2	27/2	34395.550	0.012
14	1	13	14	0	14	23/2	23/2	35153.897	0.008
						33/2	33/2	35168.391	−0.065
						25/2	25/2	35223.752	0.043
						31/2	31/2	35247.210	−0.007
						27/2	27/2	35271.881	0.024

(*continued on next page*)

Table 1 (*continued*)

J'	K_a'	K_c'	J''	K_a''	K_c''	F'	F''	Frequency	o−c
						29/2	29/2	35282.922	0.027
15	1	14	15	0	15	25/2	25/2	36121.197	0.001
						27/2	27/2	36192.370	0.076
						33/2	33/2	36214.521	−0.018
						29/2	29/2	36240.191	0.073
						31/2	31/2	36250.450	0.012
16	1	15	16	0	16	27/2	27/2	37170.792	−0.053
						37/2	37/2	37184.640	−0.038
17	1	16	17	0	17	29/2	29/2	38305.797	0.035
						39/2	39/2	38319.711	−0.020
						31/2	31/2	38379.910	0.056
						37/2	37/2	38399.813	−0.012
						33/2	33/2	38428.017	0.057
						35/2	35/2	38437.054	−0.001
18	1	17	18	0	18	31/2	31/2	39529.332	0.106
						41/2	41/2	39543.708	0.017
						33/2	33/2	39605.310	0.053
						39/2	39/2	39623.903	0.002
						35/2	35/2	39654.122	0.083
						37/2	27/2	39662.416	0.003
15	0	15	14	1	14	25/2	23/2	31283.887	0.044
						35/2	33/2	31292.693	0.122
						33/2	31/2	31348.907	−0.101
						31/2	29/2	31360.913	0.117
16	0	16	15	1	15	29/2	27/2	35654.230	0.085
						31/2	29/2	35680.099	−0.151
11	2	10	12	1	11	25/2	27/2	38451.533	−0.003
						19/2	21/2	38471.176	0.098
14	1	13	13	2	12	25/2	27/2	29644.438	−0.015
						31/2	33/2	29706.264	0.017
						21/2	23/2	29714.045	−0.014
14	2	12	15	1	15	23/2	25/2	39039.674	−0.054
						33/2	35/2	39052.717	−0.052
						31/2	33/2	39145.919	−0.122
						27/2	29/2	39172.959	−0.027
						29/2	31/2	39182.039	−0.086
15	2	13	16	1	16	27/2	29/2	36551.088	0.015
						33/2	35/2	36571.031	0.044
						29/2	31/2	36599.185	−0.131
17	2	15	18	1	18	31/2	33/2	31699.768	−0.075
						37/2	39/2	31717.613	−0.098
						33/2	35/2	31747.826	−0.124
						35/2	37/2	31755.055	−0.124
18	2	16	19	1	19	33/2	35/2	29433.019	0.066
						35/2	37/2	29480.402	−0.135
						37/2	39/2	29486.681	−0.059
28	3	26	29	2	27	61/2	63/2	31566.466	0.010
29	3	26	30	2	29	63/2	65/2	38104.262	0.081
						53/2	55/2	38118.468	−0.063
						55/2	57/2	38121.718	−0.049
						61/2	63/2	38136.847	−0.036
						57/2	59/2	38145.284	0.099
						59/2	61/2	38153.726	0.079
30	3	27	31	2	30	63/2	65/2	34939.296	0.037
						55/2	57/2	34964.426	0.040
						57/2	59/2	35057.788	0.137
31	3	28	32	2	31	67/2	69/2	31865.860	0.090
						57/2	59/2	31888.219	−0.065
						65/2	67/2	31898.883	−0.032
						63/2	65/2	31903.813	−0.112
						59/2	61/2	31906.237	−0.032
						61/2	63/2	31911.152	−0.112

Three hundred and fifteen transitions in F (89 in J_τ) with $F_{max} = 67/2$ used in the fit; rms = 0.062 MHz.

[a] Partially masked; not used in the fit.

Table 2
Rotational transitions of $I^{14}N^{15}N^{14}N$ (frequencies in MHz)

J'	K_a'	K_c'	J''	K_a''	K_c''	F'	F''	Frequency	o−c
6	2	5	5	2	4	9/2	7/2	21678.095	0.170
						15/2	13/2	21678.095	0.084
						7/2	5/2	21711.824	0.224
						17/2	15/2	21713.535	−0.008
						7/2	7/2	21845.916	0.074
6	0	6	5	0	5	17/2	15/2	21683.221	0.088
						15/2	13/2	21685.735	−0.029
6	2	4	5	2	3	9/2	7/2	21688.488	−0.015
						15/2	13/2	21689.038	0.245
						17/2	15/2	21723.663	0.062
6	3	4	5	3	3	9/2	7/2	21706.644	0.061
						17/2	15/2	21742.972	−0.009
6	4	2	5	4	1	9/2	7/2	21742.972	0.119
						7/2	5/2	21842.430	−0.272
6	3	3	5	3	2	7/2	5/2	21767.341	−0.198
6	1	5	5	1	4	15/2	15/2	21779.411	−0.548
15	2	14	16	1	15	31/2	33/2	21788.928	0.066
13	0	13	12	1	12	31/2	29/2	21860.884	0.199
7	1	7	6	1	6	11/2	9/2	24898.129	−0.025
						13/2	11/2	24901.031	−0.069
						15/2	13/2	24914.184	−0.001
						17/2	15/2	24927.983	0.011
						19/2	17/2	24928.999	0.046
7	1	6	6	1	5	15/2	13/2	25673.242	0.215
						17/2	15/2	25682.884	−0.281
						13/2	11/2	25685.105	−0.112
						11/2	9/2	25695.831	−0.202
						19/2	17/2	25705.582	0.065
7	5	2	6	5	1	15/2	13/2	25221.691	−0.076
						17/2	15/2	25252.559	−0.041
						11/2	9/2	25354.012	0.057
						19/2	17/2	25400.136	−0.178
7	4	3	6	4	2	15/2	13/2	25250.665	0.048
						11/2	11/2	25302.764	−0.344
						11/2	9/2	25328.011	−0.161
						19/2	17/2	25367.349	−0.016
						9/2	7/2	25395.550	−0.130
7	0	7	6	0	6	11/2	9/2	25258.821	−0.241
						19/2	17/2	25289.205	0.049
						9/2	7/2	25266.554	−0.046
						13/2	11/2	25267.158	−0.105
7	3	5	6	3	4	15/2	13/2	25273.760	0.069
						13/2	11/2	25282.001	0.094
						17/2	15/2	25290.464	0.118
						11/2	9/2	25309.294	0.198
						19/2	17/2	25342.014	−0.018
						9/2	7/2	25350.440	0.059
7	2	6	6	2	5	15/2	13/2	25284.608	0.050
						9/2	7/2	25313.385	0.262
						19/2	17/2	25318.724	0.131
						11/2	11/2	25427.764	−0.097
7	2	5	6	2	4	13/2	11/2	25298.378	−0.099
						15/2	13/2	25302.059	0.079
						17/2	15/2	25315.070	0.159
						9/2	7/2	25329.391	0.093
						19/2	17/2	25334.704	−0.159
						13/2	13/2	25363.052	−0.427
7	4	3	6	4	2	9/2	7/2	25395.550	−0.130
7	6	1	6	6	0	19/2	17/2	25440.091	−0.148
20	2	18	21	1	21	37/2	37/2	25624.294	−0.003

Fifty nine Transitions in F (19 in J_τ) with $F_{max} = 37/2$ used in the fit; rms = 126 kHz.

Table 3
Spectroscopic constants of iodine azide isotopomers

	$I^{14}N_3$	$I^{14}N^{15}N^{14}N$
Rotational constants (MHz)		
A	30775.669 (10)	30762.32 (24)
B	1891.0338 (5)	1861.1795 (19)
C	1779.6352 (4)	1753.1099 (45)
Centrifugal distortion constants (kHz)		
Δ_J	0.6017 (15)	0.375 (35)
Δ_{JK}	−45.028 (35)	−44.246 (94)
Δ_K	1800.0 (25)	1800.0[a]
δ_j	0.07993 (20)	0.07993[a]
δ_k	2.76 (10)	2.76[a]
κ	−0.9923	−0.9925
Quadrupole coupling constants (MHz)		
χ_{aa}	−1912.39 (17)	−1917.31 (39)
$\chi_{bb} - \chi_{cc}$	−838.16 (24)	−832.28[a]
χ_{ab}	−1656.93 (20)	−1646.4 (20)
χ_{bb}	537.11 (27)	542.6 (13)
χ_{cc}	1375.28 (15)	1374.8

[a] Values fixed to parent molecule.

calculations. The principal values should be the same within reasonable error limits for both isotopomers. This is not quite the case due to the lack of sufficient b-type transitions of the ^{15}N-species. However, the relative differences are rather small, 0.4–0.04%, confirming the correctness of the assignments. Of course, for comparisons and discussions the precise values of the parent molecule are used. The asymmetry parameter is remarkably close to zero, indicating a very symmetric charge distribution around the I–N-bond.

3.3. Structure

From Watson's [10] determinable constants the moments of inertia were calculated as given in Table 5. The inertial defect of 0.3019 amu Å^2 proves the planar arrangement of the four atoms and is typical for such a type of molecules with C_s-symmetry and consisting of only a few 'heavy' atoms: INCO 0.4441 [8], BrNCO 0.401 [11], NC–N_3 0.347 [12], FN_3 0.229 [14], and ClN_3 [15]. To describe this planar geometry five parameters are needed: three bond lengths and two bond angles. But the measurements yielded only four independent moments of inertia. However, because the quadrupole coupling tensor is so symmetric we could reasonably assume that its principal axis 'z' coincides with the direction of the I–N–bond, and therefore the angle φ is another independent quantity for the structure determination. From the six moments of inertia I_b and I_c from each species were used because these are less sensitive to vibrational effects than the small values of I_a. Two kinds of calculation have been carried out:

- The five equations expressing the four moments of inertia and the angle φ of the ^{14}N-species in terms of the parameters have been solved for these parameters.
- In addition the angle φ of the ^{15}N-species has been used to give a system of six equations. Thus, a least squares calculation for the five parameters was possible.

Both methods gave exactly the same results for the structural parameters. They are listed in Table 6 under 'Method I'. But, as pointed out in Section 4, the resulting structure is rather unusual for an azido group, and the assumption of the coincidence of χ_{zz} with the I–N-direction is obviously not quite correct. Therefore, another calculation was carried out: instead of making use of the angle φ, the distance N_b–N_c (numbering shown on Fig. 5) was fixed to the value as found in the well determined hydrazoic acid [13] and the four moments of inertia solved for the remaining four parameters. The results are also shown in Table 6 as 'Method II', the angle φ now different, and depicted in Fig. 5.

Table 4
Principal values of the quadrupole coupling tensor of iodine azide isotopomers

	$I^{14}N_3$	$I^{14}N^{15}N^{14}N$
χ_{xx}	1372.80 (9)	1367.6 (5)
χ_{yy}	1375.28 (15)	1374.8 (5)
χ_{zz}	−2748.08 (35)	−2742.4 (20)
φ[a]	26.765 (2)	26.619 (8)
η	0.0009 (2)	0.0026 (11)

[a] ∢ between quadrupole z-axis and inertia a-axis.

Table 5
Moments of inertia of iodine azide from Watson's determinable constants

	$I^{14}N_3$	$I^{14}N^{15}N^{14}N$
I_a	16.4214	16.4285
I_b	267.2556	271.5425
I_c	283.9788	288.2756
Δ	0.3019	0.3046

Ref. [10].

4. Discussion

For a structure comparison only three other covalent azides are available with reliable microwave structures without assumptions: HN_3 [13], FN_3 [14], and ClN_3 [15]. These are included in Table 6 along with the results of the electron diffraction work [6] and of the ab initio calculations [2]. As already pointed out in Refs. [14,16],

Table 6
Structure comparison of azides (distances in pm, angles in degrees)

Parameter	IN_3[a] Method I	IN_3[a] Method II	IN_3[b] El.-diffr.	IN_3[c] ab initio	FN_3[d]	HN_3[e]	ClN_3[f]
$r(X-N_a)$	215.8	209.7	212.0	213.3	144.4	101.5	174.5
$r(-N_a-N_b)$	117.9	123.8	126.0	125.8	125.3	124.3	125.2
$r(N_b-N_c)$	111.5	113.4[g]	114.7	116.7	113.2	113.4	113.3
$\sphericalangle(X-N_a-N_b)$	109.1	109.9	106.6	110.2	103.8	108.8	108.8
$\sphericalangle(N_a-N_b-N_c)$	172.2	172.3	169.6	171.4	170.9	171.3	171.9
φ[h]	26.765	28.009					

[a] This work.
[b] Ref. [6].
[c] Ref. [2].
[d] Ref. [14].
[e] Ref. [13].
[f] Ref. [15].
[g] Assumed.
[h] Angle between quadrupole z-axis and inertia a-axis.

the geometry of the azido group is rather insensitive to the adhering atom or group. It is obvious that the azido group in iodine azide calculated with 'Method I' differs considerably from that in the other compounds: both N–N-bonds are notably shorter and therefore, the whole group by 9 pm. On the other hand, the I–N-bond is longer than reasonably expected. If we instead make use of the mentioned stability of the azido group and consider the short distance N_b-N_c as the most stable one, hold it fixed, and solve for the remaining parameters as done in 'Method II', we obtain a very reasonable structure. This geometry is remarkably close to that of ClN_3. It should be mentioned that the two angles appear almost invariant against all kinds of assumptions. Especially, the deviation from linearity of the N_3-group in favour of a trans-configuration has again been clearly established: no real solution for the parameters could be found if the azido-group was forced to a linear arrangement. No error limits for the parameters have been given in this rigid rotor calculation because these are determined by the unknown vibrational effects. However, the distances should be accurate within ± 1.3 pm and the angles within $\pm 1.5°$ estimated from the uncertainty of the assumption and a contribution from the non-rigidity. The difference in φ of 1.24° between diagonalization of the coupling tensor and from the structure calculation according to 'Method II' seems negligible at first glance; but because the influence on the structure is so serious, it could be real and a hint of a divergence of the directions of χ_{zz} and the I–N-connecting line.

It is also most interesting to compare the bond characteristics of the two isoelectronic molecules iodine azide and iodine isocyanate as they become manifest in the principal values of the quadrupole coupling tensor and their derived quantities. This is done in Table 7: ionic character and π-character were calculated according to the theory of Townes and Dailey [17] as worked up in Ref. [18], shielding included. The close analogy is evident; but the numbers show that iodine azide has even less double bond and ionic character than the isocyanate.

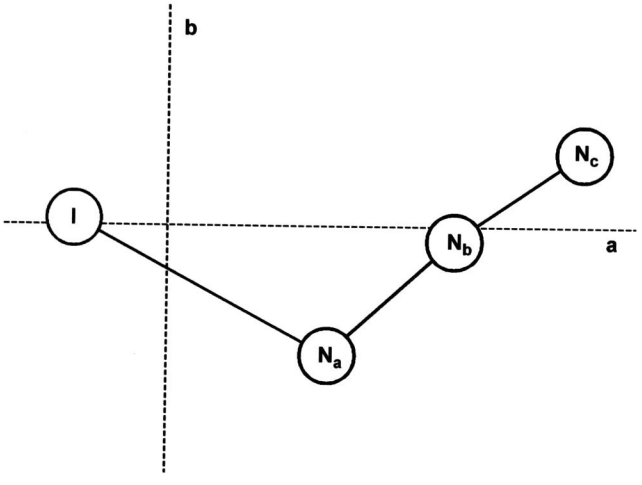

Fig. 5. Geometry of iodine azide: parameters in Table 6 under 'Method II'.

Table 7
Comparison of the I–N-bond characteristics in iodine azide and iodine isocyanate

	IN_3[a]	INCO[b]
χ_{xx}/MHz	1372.80	1499.5
χ_{yy}/MHz	1375.28	1486.58
χ_{zz}/MHz	−2748.08	−2986.1[c]
η	0.0009	−0.004
i[d] (%)	15	23
π[e] (%)	0.1	0.4

[a] This work.
[b] Ref. [8].
[c] Sign error in Ref. [8].
[d] Ionic character.
[e] π-Bond character.

Acknowledgements

We are very indebted to Prof. Dr T.M. Klapötke, Institut für Anorganische Chemie der LMU München, for suggesting this investigation, for providing materials, and for helpful discussions. We also thank Dr dr.hab. Z. Kisiel for his fitting program. The supports of the Deutsche Forschungsgemeinschaft and the Fonds der Chemischen Industrie are gratefully acknowledged.

References

[1] A. Hantzsch, Ber. Dtsch. Chem. Ges. 33 (1900) 522.
[2] P. Butzek, T.M. Klapötke, P.v.R. Schleyer, I.C. Tornieporth-Oettingand, P.S. White, Angew. Chem. Int. Ed. Engl. 32 (1993) 275.
[3] A. Schulz, I.C. Tornieporth-Oetting, T.M. Klapötke, Inorg. Chem. 34 (1995) 4343.
[4] P. Geissler, T.M. Klapötke, H.-J. Kroth, Spectrochim. Acta, Part A 51 (1995) 1075.
[5] M.-J. Crawford, T.M. Klapötke, Internet J. Vibr. Spectrosc., http://www.ijvs.com/volume3/edition6/section2.html
[6] M. Hargittai, J. Molnar, T.M. Klapötke, I.C. Tornieporth-Oetting, M. Kolonits, I. Hargittai, J. Phys. Chem. 98 (1994) 10095.
[7] H.-O. Munz, H.-K. Bodenseh, T.M. Klapötke, 14th Colloquium on High Resolution Molecular Spectroscopy, September 11–15, Dijon, France, 1995, #D16.
[8] H.M. Jemson, W. Lewis-Bevan, N.P.C. Westwood, M.C.L. Gerry, J. Mol. Spectrosc. 119 (1986) 22.
[9] H.-O. Munz, Dissertation Ulm, 1999.
[10] J.K.G. Watson, in: J.R. Durig (Ed.), Vibrational Spectra and Structure: a Series of Advances, vol. 6, Elsevier, Amsterdam, 1977, pp. 1–89.
[11] H.M. Jemson, W. Lewis-Bevan, N.P.C. Westwood, M.C.L. Gerry, J. Mol. Spectrosc. 118 (1986) 481.
[12] C.C. Costain, H.W. Kroto, Can. J. Phys. 50 (1972) 1453.
[13] B.P. Winnewisser, J. Mol. Spectrosc. 82 (1980) 220.
[14] D. Christen, H.G. Mack, G. Schatte, H. Willner, J. Am. Chem. Soc. 110 (1988) 70.
[15] R.L. Cook, M.C.L. Gerry, J. Chem. Phys. 53 (1970) 2525.
[16] N. Heineking, M.C.L. Gerry, Z. Naturforsch. 44a (1989) 669.
[17] C.H. Townes, B.P. Dailey, J. Chem. Phys. 17 (1949) 782. B.P. Dailey, C.H. Townes, J. Chem. Phys. 23 (1955) 118.
[18] W. Gordy, R.L. Cook, Microwave molecular spectra, in: A. Weissberger (Ed.), Technique of Organic Chemistry, second ed., vol. IX, Interscience Publishers, New York, 1970, pp. 551–616.